

Structural and Electronic Properties of Metal-Encapsulated Silicon Clusters in a Large Size Range

Jing Lu^{1,2,*} and Shigeru Nagase^{1,†}

¹*Department of Theoretical Studies, Institute for Molecular Science, Okazaki 444-8585, Japan*

²*Mesoscopic Physics Laboratory, Department of Physics, Peking University, Beijing 100871, People's Republic of China*

(Received 2 July 2002; published 19 March 2003)

Structural and electronic properties of metal-doped silicon clusters MSi_n s ($M = \text{W, Zr, Os, Pt, Co}$, etc.) in a large size range of $8 \leq n \leq 20$ are investigated via *ab initio* calculations. Different from a recent experimental suggestion that the metal atom is endohedral in MSi_n , we reveal that the formation of endohedral structure strongly depends on the size of the Si_n cluster. Two novel structures of the chemically stable endohedral species are manifested. The suitable $M@Si_n$ building blocks of self-assembly materials vary in the range of $10 \leq n \leq 16$. The thermodynamical magic numbers are found to coincide with the chemical magic numbers for five clusters.

DOI: 10.1103/PhysRevLett.90.115506

PACS numbers: 61.46.+w, 36.40.Cg, 82.60.Qr

The basis to fabricate cluster-assembled nanostructures is to find out suitable building blocks that are chemically stable and weakly interact with each other. Silicon clusters are expected to become such a building block in light of the extreme importance of silicon in the semiconductor industry. However, pure silicon clusters are chemically reactive [1] due to a universal existence of dangling bonds (DBs) [2–4] and are unsuitable as a building block of self-assembly materials. This status is now dramatically changed by introducing a metal atom in the Si_n clusters. A reaction of silane (SiH_4) with transition metal ions M^+ ($M = \text{Hf, Ta, W, Re, Ir}$, etc.) has led to MSi_nH_x clusters that only have a smaller number of hydrogens ($x \leq 4$ for all n). Especially completely dehydrogenated MSi_n clusters appear at $n = 14, 13, 12, 11$, and 9, respectively, as an end product. The smaller hydrogen content in the MSi_nH_x clusters implies that most or all Si dangling bonds have been saturated by the M atom. To play that role, the M atom is conjectured to be located in the center of Si_n clusters [5], and a subsequent *ab initio* calculation identified a regular hexagonal prism with the W on the center as the ground state of WSi_{12} . There are several essential open questions about the MSi_n clusters. (1) Is the metal atom always located in the center of the Si_n clusters? (2) What is the size range of the chemically stable MSi_n clusters? (3) Why do the MSi_n cluster growths end at those specific numbers [5]?

As an effort to address the above questions, here we provide an *ab initio* structural and electronic investigation for transition-metal-doped silicon clusters MSi_n s ($M = \text{W, Zr, Os, Pt, Co}$, etc.) in a large size range ($8 \leq n \leq 20$). The calculations are performed within the spin-unrestricted hybrid density functional theory with the B3LYP (Beck three-parameter Lee-Yang-Parr) exchange-correlation functional [6]. Pure and polarized double zeta basis set, labeled by LanL2DZ and LanL2DZ(d), are adopted for the M and Si atoms, respectively. The effective core potentials that have included the relativistic effects for the second and third

transition series are used for all the atoms [7]. In order to check basis effects, a larger all-electron polarized triple zeta basis set plus one diffuse function, labeled by 6-311 + $G(d)$, is employed for the Si atom in single point energy calculations for several MSi_n clusters, and the energetic orderings of the competitive isomers are essentially unchanged except for $Os@Si_{14}$. The Si_n isomers selected to construct the initial MSi_n clusters are summarized in Table I. They have either lower energies or higher symmetries so that each Si atom has a chance to bond to the M atom. Harmonic vibrational frequencies are calculated for the promising stationary points from a direct structural optimization, and reoptimization is performed following the eigenvector of the first imaginary frequency for the saddle point if any until a local energy minimum is finally achieved. The embedding energy (EE) of M inside or outside Si_n is defined as $EE = E[Si_n] + E[M] - E[MSi_n]$, and $E[Si_n]$ is the energy of the most stable Si_n isomer [3,4]. The Kohn-Sham energy gap between the highest occupied molecular orbital (HOMO) and lowest unoccupied molecular orbital (LUMO) is calculated using the nonhybrid BLYP functional to keep comparison with other calculations [9–11]. A chemically stable M -doped Si_n cluster satisfies three conditions herein: a full protection of the M atom (i.e., an endohedral structure), an absence of Si DBs, and a large HOMO-LUMO gap of over 0.50 eV valid for the carbon fullerenes [11,12]. The cutoff distances for the M -Si and Si-Si bonds are defined at 2.93 and 2.70 Å, respectively.

The calculated properties of the lowest energy isomers of the M -doped Si_n clusters are partially given and compared with the experimental data [5] in Table II. The lowest energy geometries of the W-doped Si_n clusters are displayed in Fig. 1, and those of the M -doped Si_n clusters that satisfy the octet rule [5] but $M \neq$ group 6 metals are displayed in Fig. 2. At first glance, three clusters, WSi_8 , $PtSi_8$, and $CoSi_9$, are exohedral species. The exohedral WSi_8 has no Si DBs and is expected magic in the stability against H, which is in good agreement

TABLE I. Si_n isomers used for constructing the initial $M\text{Si}_n$ clusters. Two routines are employed to construct $M@Si_{18}$: capping two faces of $M@Si_{16}$ or removing two capping atoms of $M@Si_{20}$. *tri*: trigonal; *tetra*: tetragonal; *p*: pentagonal; *b*: basketlike; *h*: hexagonal; *c*: cubic; *d*: decahedral; *f*: fullerene-like; *hp*: heptagonal; *FK*: Frank-Kasper.

	Isomers
Si_8 [8]	D_{3d} bicapped octahedron, C_{2v} and C_{3v} tetracapped tetrahedrons, C_{2v} bicapped <i>tri</i> prism, D_{4h} <i>tetra</i> prism, D_{4d} <i>tetra</i> antiprism
Si_9 [8]	C_{3v} tricapped octahedron, D_{3h} tricapped <i>tri</i> prism
Si_{10} [8]	D_{5h} <i>p</i> prism, D_{5d} <i>p</i> antiprism, T_d tetracapped octahedron, C_{3v} tetracapped <i>tri</i> prism, D_{4d} bicapped <i>tetra</i> antiprism
Si_{12} [3,5]	<i>b</i> structure, C_{2v} hexacapped <i>tri</i> prism, D_{6h} <i>h</i> prism, D_{6d} <i>h</i> antiprism, I_h icosahedron
Si_{14} [9]	<i>c</i> , <i>d</i> , and <i>f</i> structures, D_{7h} <i>hp</i> prism, D_{6h} bicapped <i>h</i> prism
Si_{15} [10]	<i>f</i> , <i>c1</i> , and <i>c2</i> structures
Si_{16} [9]	<i>f</i> and <i>FK</i> structures, tetracapped <i>h</i> prisms
Si_{20}	I_h dodecahedron

with an observed local maximum relative abundance of WSi_n among WSi_nH_x at $n = 8$ (about 30%) [5]. The calculated energy differences between the exohedral WSi_n and endohedral W@Si_n are $\Delta E = E_{\text{exo}} - E_{\text{endo}} = -0.50, 0.39, 1.63,$ and ≈ 6 eV (estimated from an exohedral D_{6h} structure) for $n = 8, 9, 10,$ and $12,$ respectively, indicative of an enhanced thermodynamic stability of the endohedral structure against the exohedral one with the increased size. The cause lies in that the *M*-Si bond number in the endohedral structure increases more quickly than that in the exohedral one with the increased

size. A clear exohedral-endohedral structural transition with the increased size has been recently observed in the W- and Tb-doped Si_n clusters [13], and the smallest endohedral W@Si_n clusters are shown to be W@Si_{10} , only one size larger than our prediction. Hence, from $n = 12,$ we no longer consider exohedral cases.

The chemically stable $M@Si_n$ clusters in our calculations spread from $n = 10$ to $n = 16$. The smallest chemically stable $M@Si_n$ cluster is attributed to a basketlike Os@Si_{10} , which stems from the C_{3v} tetracapped trigonal prism and have Os-Si and Si-Si bond lengths of

TABLE II. Theoretical ($\text{NDB}_{\text{theor}}$) and experimental number (NDB_{expt}) [5] of Si DBs, HOMO-LUMO gaps (eV), chemical stability, EE (eV), BE (binding energy, in eV/atom), and natural charges on *M* for the *M*-doped Si_n clusters. The capital letters *L* and *H* represent lower and higher chemical stability, respectively. Fe@Si_{10} has a magnetic moment of $2\mu_B$ while for all others it is zero. All the Pt@Si_n and larger-size $M@Si_n$ ($n = 17$ [10], 18, and 20) always have Si DBs.

<i>M</i> -doped Si_n	$\text{NDB}_{\text{theor}}$	NDB_{expt}	Gap	Chemical stability	EE	BE	Charge
WSi_8	0	0	0.95	<i>L</i>	5.43	3.44	-0.41
PtSi_8	11	...	1.38	<i>L</i>	4.35	3.33	-0.10
W@Si_9	9	nonzero	1.19	<i>L</i>	5.14	3.42	-2.14
CoSi_9	1	0	0.34	<i>L</i>	3.96	3.12	0.49
W@Si_{10}	6	nonzero	1.39	<i>L</i>	5.09	3.50	-1.74
Os@Si_{10}	0	...	1.48	<i>H</i>	5.60	3.55	-1.19
Ru@Si_{10}	2	...	0.72	<i>L</i>	4.21	3.42	-1.26
Fe@Si_{10}	0	...	0.25	<i>L</i>	2.27	3.25	-0.80
W@Si_{12}	0	0	1.38	<i>H</i>	8.64	3.69	-1.74
Zr@Si_{12} (C_1)	8	nonzero	0.78	<i>L</i>	4.81	3.40	-0.45
Os@Si_{12} (D_{6h})	0	...	1.10	<i>H</i>	8.36	3.67	-1.28
W@Si_{14} (<i>f</i>)	0	...	0.38	<i>L</i>	8.74	3.70	-1.98
Zr@Si_{14} (<i>dbhpa</i>)	1	0	0.65	<i>L</i>	6.34	3.54	-1.97
Zr@Si_{14} (<i>dbhpb</i>)	0	0	1.23	<i>H</i>	6.18	3.53	-2.13
Os@Si_{14} (<i>c</i>) ^a	0	...	1.63	<i>H</i>	7.19	3.60	-1.68
W@Si_{15} (<i>f</i>)	0	...	0.79	<i>H</i>	10.06	3.71	-2.04
W@Si_{16} (<i>f</i>)	1	...	1.11	<i>L</i>	10.22	3.73	-2.13
Zr@Si_{16} (<i>f</i>)	0	...	1.52	<i>H</i>	9.59	3.69	-2.19
$\text{W}_2@Si_{20}$	0	...	0.55	<i>H</i>	16.75	3.65	-1.95

^aObtained using the 6-311 + $G(d)$ basis set for the Si atom, while the LanL2DZ(*d*) basis set prefers the *dbhpa* structure.

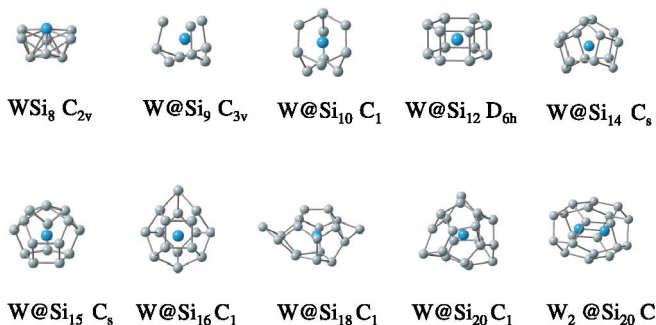


FIG. 1 (color). Ground state isomers of the W-doped Si_n clusters and $\text{W}_2@Si_{20}$. The light blue balls represent Si atoms. For the endohedral structures, bonds connecting the W to the Si atoms are not displayed for clarity. The structures of $\text{Mo}@Si_{12}$ and $\text{Cr}@Si_{12}$ are identical with that of $\text{W}@Si_{12}$. The $\text{Os}@Si_{15}$ and $\text{Zr}@Si_{16}$ have compact f structures, while $\text{Pt}@Si_{14}$, $M@Si_{15}$ ($M = \text{Zr}$ and Pt), and $M@Si_{16}$ ($M = \text{Os}$ and Pt) have distorted or capped f structures. All the larger-size $M@Si_n$ ($n = 17$ [10], 18, and 20) clusters have capped cage structures.

2.39–2.49 Å and 2.36–2.48 Å, respectively. The lowest energy isomer of $\text{Zr}@Si_{14}$ is a C_1 distorted bicapped hexagonal prismatic (*dbhpa*) structure, originating in the d structure and having two bonded capping atoms. However, a presence of one DB on its most projecting Si atom is contradictory to the observed higher stability against H for $\text{Zr}@Si_{14}$ [5]. Starting from the D_{6h} bicapped h prism, one can obtain a D_{2h} distorted bicapped hexagonal prismatic (*dbhpb*) structure with two well-separated capping atoms. It is 0.16 eV slightly higher in energy than the *dbhpa* structure, but has no Si DBs. Keep in mind that the actual reaction between the metal and silicon is performed in the high-temperature vapor phase [5,13,14], where the entropy effect probably becomes as important as that observed for carbon clusters [15]. The free energy is calculated as the expressions given in Ref. [16]. The results show that, above 1200 K, the *dbhpb* structure indeed becomes more stable than the *dbhpa* one. The Zr-Si and Si-Si bond lengths are in the ranges of 2.72–2.93 Å and 2.28–2.42 Å, respectively, in the *dbhpb* structure.

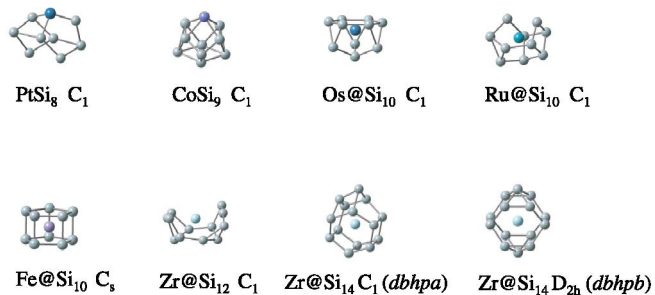


FIG. 2 (color). Ground state isomers of the M -doped Si_n clusters that satisfy the octet rule but $M \neq$ group 6 metals with the one exception of $\text{Zr}@Si_{12}$

The even charge distribution in the region between the Os and the six Si atoms on the hexagonal ring in $\text{Os}@Si_{10}$ [Fig. 3(a)] shows a metallic bonding between them, while a covalent bonding is clear between the Os and the bottom Si atoms from the high charge density along them [Fig. 3(b)]. In $\text{Zr}@Si_{14}$, the covalent character appears in the four shortest Zr-Si bonds, one of which is displayed in Fig. 3(c). From Table II, the average natural charges are about -2 for the W and Zr atoms and -1 for the Os atom, respectively. Hence, the bonding between the Os atom and the Si_{10} cage is a mixture of metallic, covalent, and ionic bonding, whereas the one between the Zr atom and the Si_{14} cage is a mixture of the two latter bonding. Consequently, a strong interaction between the Os (Zr) atom and the Si_{10} (Si_{14}) cage is anticipated, as is confirmed from the large EEs of the Os (5.60 eV) and Zr atom (6.18 eV) inside Si_{10} and Si_{14} , respectively.

Figure 4 shows the size dependences of the EEs and BEs of the M -doped Si_n clusters ($M = \text{W}$, Zr, Os, and Pt). Initially, the four BEs generally increase with the increased size, simultaneously peaking at $n = 16$. Besides $n = 16$, special thermodynamical stability is also seen at $n = 8$ and 12 for $M = \text{W}$, $n = 14$ for $M = \text{Zr}$ and Pt, and $n = 12$ for $M = \text{Os}$. If the M and Si are fully reacted, the strongest abundance can be anticipated at the global thermodynamically stable point, i.e., $n = 16$, for all the four clusters (for $M = \text{W}$, a comparable abundance can also be anticipated at $n = 15$ due to its close BE to the case of $n = 16$). However, in an incomplete reaction, the cluster growth would probably end at smaller-size locally thermodynamically stable points. Compared with previous separate calculations [10,17], our job first gave a unified explanation to the observed cluster growth end at $n = 12$ [5] and strongest abundance at $n = 15$ and 16 [14] for the W-doped Si_n clusters when using the inert silane and reactive bare Si atoms or clusters as Si source, respectively. The observed cluster growth end at $n = 14$ for the Zr-doped Si_n clusters corresponding to using the silane as Si source can be well understood in the same way. The EE- n curves have much similarity to the BE- n ones. Initially, the four EEs generally increase with the increased size owing to the increased M -Si bond number,

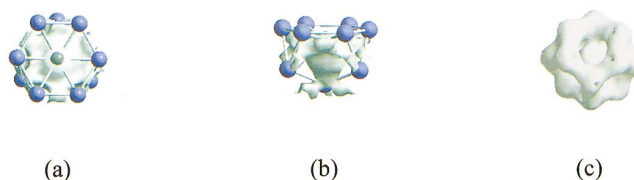


FIG. 3 (color). Constant electronic charge density surfaces for (a) $\text{Os}@Si_{10}$ viewed from the top of the hexagonal plane, (b) same as (a) but viewed from the side of the hexagonal plane, and (c) for the *dbhpb* $\text{Zr}@Si_{14}$. The charge densities at the surfaces are 0.060 and 0.045 a.u. for $\text{Os}@Si_{10}$ and $\text{Zr}@Si_{14}$, respectively.

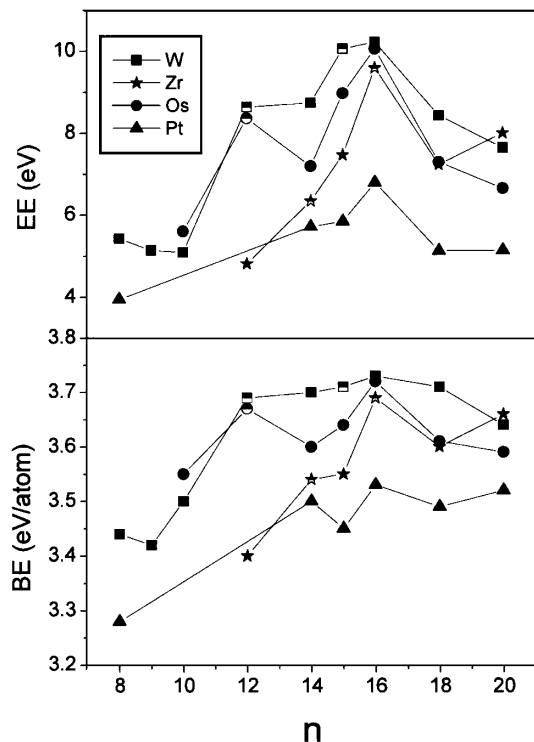


FIG. 4. Size dependences of the EEs and BEs of the M -doped Si_n with $M = \text{W}, \text{Zr}, \text{Os},$ and Pt . The clusters with simultaneous special thermodynamical and chemical stabilities are labeled by half-filled signs.

and they simultaneously peak at $n = 16$ as well. This suggested that the maximal coordination of M with Si is 16, a result consistent with the observed size upper limit of the compact $M@Si_n$. To stabilize higher Si_n clusters, more metal atoms are thus required. Optimization of the Si_{20} fullerene containing a W dimer can indeed result in a compact elongated dodecahedron (Fig. 1). Remarkably, the locally stable points in the BE- n curves are also the ones in the EE- n curves except for $\text{Zr}@Si_{14}$, and this correspondence indicates that the locally thermodynamical stability arises from an exceptionally strong interaction between the M and the Si_n cage at these points. Notably five clusters are found to show high both chemical and thermodynamical stabilities, and they are $\text{W}@Si_{12}$, $\text{W}@Si_{15}$, $\text{Zr}@Si_{14}$, $\text{Zr}@Si_{16}$, and $\text{Os}@Si_{12}$.

In summary, the metal atom is not always located in the center of the Si_n clusters even for the completely dehydrogenated species, unless the sizes of the Si_n clusters are large enough. Two novel structures of the chemically stable $M@Si_n$ s (basketlike structure for $\text{Os}@Si_{10}$ and distorted bicapped hexagonal prism for $\text{Zr}@Si_{14}$) are

revealed for the first time, and the suitable $M@Si_n$ building block for cluster-assembled materials is distributed in the range of $10 \leq n \leq 16$. There are simultaneous magic behaviors in thermodynamical and chemical stabilities for $\text{W}@Si_{12}$, $\text{W}@Si_{15}$, $\text{Zr}@Si_{14}$, $\text{Zr}@Si_{16}$, and $\text{Os}@Si_{12}$, which agree well with the experimental growth end at $n = 12$ and 14 in a dehydrogenated form for the W- and Zr-doped Si clusters, respectively [5].

All the calculations were done using the GAUSSIAN 98 package [18]. This work was supported by the JSPS, NSFC (Grant No. 10104001), and TWAS. We thank Professor V. Kumar for providing the geometry of one cubic $\text{W}@Si_{15}$ and Y. Zhou, Y. Choe, S. Re, N. Takagi, S. Zhang, and Y. Wu for helpful discussions.

*Electronic address: lu@ims.ac.jp

†Electronic address: nagase@ims.ac.jp

- [1] For example, see M. F. Jarrold and J. E. Bower, *J. Chem. Phys.* **96**, 9180 (1992), and references therein.
- [2] U. Rothlisberger, W. Andreoni, and M. Parrinello, *Phys. Rev. Lett.* **72**, 665 (1994).
- [3] K. M. Ho *et al.*, *Nature* (London) **392**, 582 (1998).
- [4] I. Rata *et al.*, *Phys. Rev. Lett.* **85**, 546 (2000).
- [5] H. Hiura, T. Miyazaki, and T. Kanayama, *Phys. Rev. Lett.* **86**, 1733 (2001).
- [6] A. D. Beck, *J. Chem. Phys.* **98**, 5648 (1993).
- [7] P. J. Hay and W. R. Wadt, *J. Chem. Phys.* **82**, 270 (1985); **82**, 299 (1985); W. R. Wadt and P. J. Hay, *ibid.* **82**, 284 (1985).
- [8] K. Raghavachari and C. M. Rohlfing, *J. Chem. Phys.* **89**, 2219 (1988).
- [9] V. Kumar and Y. Kawazoe, *Phys. Rev. Lett.* **87**, 045503 (2001).
- [10] V. Kumar and Y. Kawazoe, *Phys. Rev. B* **65**, 073404 (2001).
- [11] B. L. Zhang *et al.*, *J. Chem. Phys.* **98**, 3095 (1993).
- [12] F. Diederich *et al.*, *Science* **252**, 548 (1991).
- [13] M. Sanekata *et al.*, *Trans. Mater. Res. Soc. Jpn.* **25**, 1003 (2000); M. Ohara *et al.*, *J. Phys. Chem. A* **106**, 3702 (2002).
- [14] S. M. Beck, *J. Chem. Phys.* **87**, 4233 (1987); **90**, 6306 (1989).
- [15] J. M. L. Martin, J. El-Yazal, and J.-P. Francoïş, *Chem. Phys. Lett.* **248**, 345 (1996).
- [16] D. A. McQuarrie, *Statistical Thermodynamics* (Harper & Row, New York, 1973).
- [17] S. N. Khanna, B. K. Rao, and P. Jena, *Phys. Rev. Lett.* **89**, 016803 (2002).
- [18] M. J. Frisch *et al.*, *Gaussian 98 Revision A.9* (Gaussian, Inc., Pittsburgh, PA, 1998).